HANSER

Precision Injection Molding

Jehuda Greener, Reinhold Wimberger-Friedl

Process, Materials and Applications

ISBN 3-446-21670-7

1 Precision Injection Molding: Overview and Scaling Considerations

J. Greener and R. Wimberger-Friedl

1.1 Introduction

With the explosive growth in information technology over the past three decades and the advent of mass-produced information storage devices (e.g., CD, CD-ROMs and DVD), and other related products much attention has been given to the injection molding process as the most cost-effective and agile processing technology for manufacturing such demanding components on a mass scale. Also, microfluidic devices for medical diagnostics have recently created a new demand for injection molded precision parts. One of the key aspects of the production of such articles is the need to meet extremely tight dimensional tolerances—typically in the submicron range—and maintain these tolerances over the practical lifetimes of the molded articles. In addition, because many of the precision components are utilized in various optoelectronic applications, control of optical and electrical properties is often crucial.

The strict control of the geometric and functional features of precision components requires a systematic reexamination of the conventional injection molding (CIM) process with special consideration of its impact on the dimensions and electro-optical characteristics of the molded article. We will show, in fact, that precision injection molding (PIM) is a special subclass of the conventional process with a distinct set of design, processability, and optimization criteria. This volume examines precision injection molding from different perspectives, covering materials, process, and hardware with a special emphasis on the dimensional integrity and stability of the molded components. In the sections below we provide a general framework and key definitions for discussion and examination of PIM technology.

1.2 The M-Chain of Precision Molding

The attainment of tight dimensional and functional tolerances requires a complete—from the ground up—examination of the injection molding operation following the so-called M-chain of precision molding*:

* This term was coined during the precision-molding project at Philips PMF in the late 1980s.

- *M*an/operator
- *M*achine
- *M*old
- *M*ethod
- *M*aterial

While most operations today are fully automated and robotics is widely utilized, the presence of a skilled operator ("*man*") is essential for high precision applications, when operating at the edge of the capabilities of injection molding technology. These operations are characterized by a very tight process window, where continuous monitoring and frequent intervention may be required to meet the demanding specifications of the corresponding products. High precision operations require close attention to detail and involve such diverse functions as material specification and handling, mold design, machine design, system operation and maintenance, clean room operations, and product handling and certification. All of these functions require skilled and experienced operators.

The *machine* is another key element in the chain. The machine is responsible for melting and plasticating the material and precisely and reproducibly metering the molten resin into the mold. This requires tight control on temperature, displacement volume, and injection speed, and fast and reproducible changeover from injection to packing (section 1.3). PIM machines are generally distinguished by precision machining and sophisticated closed-loop control systems used to deliver the necessary injection accuracy and reproducibility (chapters 10 and 11 [1, 2]). Micro-molding machines, designed to handle small injection volumes and precise displacement, are typically used for very small parts (chapter 9 [3]). These machines utilize somewhat different process control algorithms compared to more standard PIM machines because of the very small displacement volumes and thermal loads associated with these operations.

The *mold* is another crucial element in the M-chain. All parts and inserts of the mold must meet precise machining and assembling tolerances (chapters 8 [4] and 11 [2]). Additionally, it is important to ensure that the temperature of the mold is uniform and stable throughout the molding cycle, through careful design and maintenance of the mold cooling/heating system as well as close monitoring and control of mold temperature. When hot material is injected into the mold, it tends to expand perpendicular to the parting line, causing the two mold halves to separate in response to the hydrodynamic force exerted by the injected melt. The mold must be sufficiently stiff to minimize this displacement and prevent fluctuations in cavity dimensions cycle-to-cycle while maintaining the desired dimensional tolerances for the molded article.

Different types of molding operations (*methods*) are often considered for molding precision parts. The first type is the conventional molding process wherein a hot melt is injected into a relatively cold mold in which the final part is formed. In this process the mold is essentially "passive," in the sense that it does not contribute independently to the pressure within the mold cavity. A common variant of the conventional process is the so-called hybrid or injection-compression molding process in which pressure can be applied directly in the mold cavity (in a manner akin to compression molding) and independently of the molding machine [5]. In this case the mold is said to be "active." This latter process is considered more effective in replicating very fine surface features as in the case of the compact disc (section 1.3 and

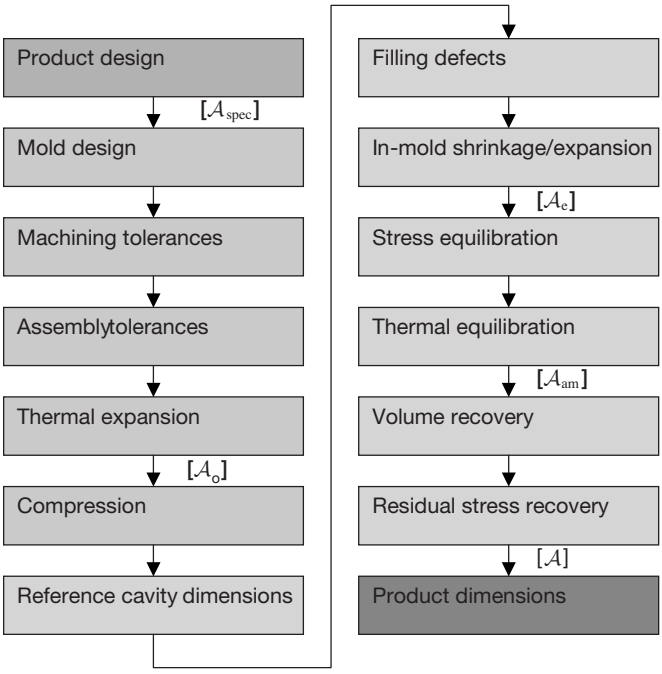

Figure 1.1: From product design to finished component: design and process steps of the M-chain of precision molding

chapter 4 [6]). Other variations of the conventional process (e.g., gas- or water-assist injection molding [7]) are also used to minimize shrinkage, sink marks, and other surface defects. In these processes carbon dioxide or water are typically co-injected into the mold to equalize and better control the pressure inside the mold cavity during the packing phase (section 1.3). Other modifications of the process with important implications for the achievable precision are two-component molding and over-, outsert-, and insert-molding [8]. All of these processes are capable of improving the dimensional integrity of the part since the effective shrinkage of the polymer is lowered by the presence of a preformed insert.

Finally, a key element of the M-chain is the *material*. Material (polymer) properties control both the processability and manufacturability of the molded article as well as its final attributes and functional performance. Mold shrinkage is one measure of the ability of a given material to accurately replicate fine features and meet tight dimensional tolerances (section 1.3). Typically, amorphous polymers exhibit lower shrinkage (0.3–0.8 %) than semi-crystalline polymers (1–3 %) [9]. The indicated values do not represent the best one can achieve with the given materials but it rather expresses the general level of difficulty in meeting tight dimensional specifications with the corresponding material type. Thus, it is clear that amorphous polymers are most suitable for PIM operations, although other material classes should not be, and, in fact, are not, excluded. It is known, for example, that shrinkage and other dimensional characteristics of the material can be substantially improved by the addition of inorganic fillers [10].

Dimensional stability, however, is generally enhanced with an increase in the glass transition temperature (T_g) of the polymer (chapter 2 [11] and section 1.4) relative to the service temperature of the part. Thus, high-T_g, amorphous polymers filled with an inorganic filler (nano- or micro-particles might be considered) would seem to offer the best dimensional stability, although the melt rheology, processability, and optical properties of such materials could be compromised, depending on the application.

A qualitative diagram representing the various steps and issues involved as we move from the product design phase to the final precision part is shown in Fig. 1.1. The final dimensions of the molded article can be influenced by many factors. The main steps affecting precision molds are listed on the left side of the diagram. The actual configuration (shape and dimensions) of the cavity at the instant of filling is generally considered as the reference configuration relative to changes occurring during the filling, packing, and cooling stages (section 1.3), which are listed on the right side of the diagram along with effects associated with the time-dependent response of polymers, such as strain recovery and physical aging. These material and process issues, relevant to PIM technology, are discussed in more detail in the following sections.

1.3 Dimensional Integrity

The configuration (shape and dimensions) of a molded part is intimately related to the thermo-mechanical history of the material in the mold cavity during the process cycle, the cavity geometry, the physical properties (particularly the compressibility and thermal expansion coefficient) of the material, and the environmental conditions and stresses applied on the part during its functional lifetime outside the mold. The configuration of the molded part can be generally decoupled into two main contributions: (a) the "as-molded" configuration (*dimensional integrity*) and (b) changes in configuration over time (*dimensional stability*). The as-molded configuration is determined by the state of the material in the mold cavity at the instant just prior to mold opening, the abrupt changes in pressure and stress upon ejection, and the subsequent unconstrained cooling of the solid part to ambient temperature after ejection from the mold. The final configuration of the as-molded part is controlled by several distinct, though strongly coupled, factors, including the pressure and temperature histories in the mold cavity, cooling (thermal) stress, warpage, and shrinkage.

The *pressure history (in-cavity pressure)* is imposed on the material during the molding cycle and is closely associated with several process parameters (e.g., injection pressure, holding/packing pressure, shot size, clamping force, injection rate), but its evolution over time depends on the cavity geometry, the temperature history of the material inside the cavity, and the thermal expansion coefficient and compressibility of the material. *Cooling (thermal) stress* is induced by the inhomogeneous cooling and solidification of the material in the cavity during the molding cycle, and it may lead to severe distortion of the as-molded part if not properly accounted for. *Warpage* relates to the distortion induced by the inhomogeneous shrinkage and relaxation of residual stress in the part once outside the mold, while *shrinkage* simply expresses the overall dimensional change as the unconstrained part cools down to ambient temperature.

The configuration of the molded part can be represented by the functional

$$\mathcal{A} = \mathcal{A}\,(\mathcal{A}_o, P, T; t) \tag{1.1}$$

where P and T are the spatially inhomogeneous pressure and temperature histories, and $\mathcal{A}_o$ is the cavity geometry. This configuration can be decoupled into two distinct contributions:

$$\mathcal{A} = \mathcal{A}_{am} + \Delta\mathcal{A}(t) \tag{1.2}$$

where $\mathcal{A}_{am}$ is the as-molded configuration, and $\Delta\mathcal{A}(t)$ expresses the change in configuration over time brought about by various material and environmental factors discussed in section 1.4. $\mathcal{A}_{am}$ can be further decomposed into two components

$$\mathcal{A}_{am} = \mathcal{A}_e + \Delta\mathcal{A}_s \tag{1.3}$$

where $\mathcal{A}_e$ is the configuration of the part at the end of the molding cycle, immediately after the part is ejected from the mold (i.e., at $t \sim t_e^+$, see Fig. 1.2) and $\Delta\mathcal{A}_s$ is the change in configuration caused by shrinkage, warpage and related phenomena as the part cools freely from its terminal temperature at the end of the cycle, T_e, to ambient (T_{amb}). $\mathcal{A}_e$ is controlled by the relief of residual stresses and the abrupt decompression as the solid part is forced to eject from the mold cavity. If the desired configuration is $\mathcal{A}_{spec}$ and the tolerance is ε, we require that

$$\mathcal{A} - \mathcal{A}_{spec} \leq |\varepsilon| \tag{1.4}$$

The tolerance is typically specified by the product designer and is expected to be quite small in PIM operations.

1.3.1 Pressure History

One of the most critical process functions in PIM is the in-cavity pressure history. To understand the role of in-cavity pressure, it is useful to examine a typical pressure history as recorded inside a mold cavity during the injection molding cycle (Fig. 1.2). As shown, the cycle can be divided into two phases: (i) filling, which is governed by the hydrodynamics of the melt flowing into the cavity as the material is injected into the mold and (ii) post-filling, which commences as soon as the cavity is completely filled and is controlled by heat transfer in the mold cavity and the compressibility of the solidifying melt. The latter can be further divided into two stages: (1) packing, for $t_{fill} < t < t_{gf}$, and (2) cooling, for $t_{gf} < t < t_e$. The post-filling phase is usually characterized by large and abrupt changes in pressure and temperature inside the mold cavity. During the packing stage, the pressure grows rapidly, under nearly isothermal conditions, to some high value, P_p, which is usually held for only a short interval and is controlled by the hold pressure applied by the machine hydraulics. At t_{gf} (the "gate freeze-off" time) the material in the gate area solidifies, and the material becomes effectively locked inside the cavity and physically isolated from the injection molding machine. After t_{gf}, the heat transfer to the mold surfaces and the compressibility of the material lead to a monotonous decay in pressure until

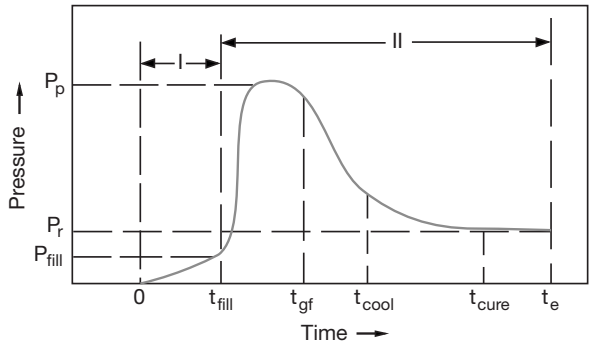

Figure 1.2: A schematic in-cavity pressure history

the termination of the cycle at t_e wherein the mold opens and the solidified part is ejected. t_{cool} and t_{cure} mark two important events during the cooling stage. At t_{cool} the material at the innermost point in the cavity passes through the glass transition temperature, T_g (for this discussion, we consider only amorphous polymers, although similar arguments can be applied to semi-crystalline polymers or thermosets), i.e., at $t > t_{cool}$ the material in the cavity is fully vitrified though not yet equilibrated to the mold temperature ($T_{mold} < T \leq T_g$). At t_{cure}**, the system approaches a thermal steady state, i.e., the temperature becomes evenly distributed throughout the cavity space ($T \approx T_{mold}$), and the pressure approaches an asymptotic value, P_r, the residual pressure. If the cycle is terminated before complete vitrification ($t_e < t_{cool}$) or even before thermal equilibration ($t_e < t_{cure}$), the part is likely to distort and warp in the subsequent free-cooling stage (cooling outside the mold from T_e to ambient) as a result of the ensuing inhomogeneous shrinkage. Similarly, if P_p is too low (insufficient packing), the pressure in the cavity will go to zero at $t < t_{cure}$ and the material will delaminate from the cavity walls before t_e (the *terminal time*), leading to inadequate replication of the cavity geometry. Several qualitative packing scenarios and corresponding trajectories on the volume-temperature space of the material are illustrated in Fig. 1.3. General criteria for selecting P_p and t_e and their impact on the part configuration are discussed elsewhere [12].

While the pressure could directly impact the part geometry, the complete thermo-mechanical history (i.e., the time evolution of pressure, temperature, and deviatoric stress) controls the thermodynamic state of the molded material, which carries some implications for the dimensional stability of the part (section 1.4). Because of the general spatial nonuniformity of the thermo-mechanical history within the cavity, injection molded parts are inherently inhomogeneous [13, 14], which could lead to inferior dimensional integrity and poor dimensional stability. This inherent deficiency can be practically mitigated by using a hybrid (injection-compression) molding process [5], whereby the pressure in the cavity during the post-filling stage is held at a constant level and is spatially uniform. This process requires an "active" mold and it involves a switchover from an injection to a compression mode at the beginning of

**This is a misnomer as there are typically no curing reactions during the molding cycle. This term, however, is commonly used by molding engineers and machine operators.

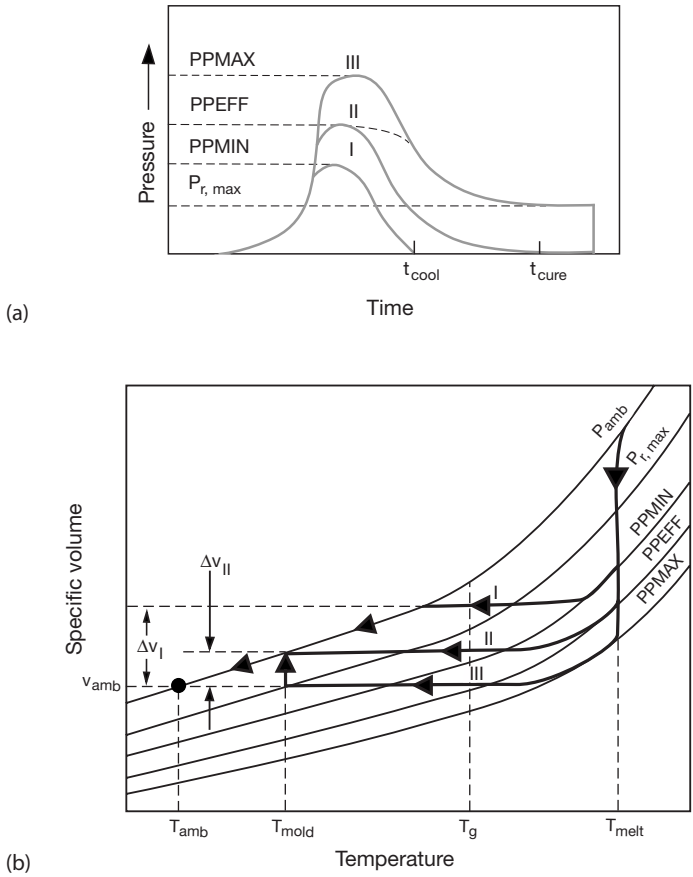

Figure 1.3: (a) Three packing scenarios and (b) corresponding trajectories on the volume-temperature space of the material [12]

the packing phase, whereby the pressure in the cavity becomes constant while the volume (thickness) of the cavity decreases as the material cools down.

1.3.2 Cooling Stresses

Residual cooling (thermal) stresses are an inherent feature of the injection molding process with a potentially detrimental effect on the dimensional integrity and stability of the molded part. These stresses are induced by the inhomogeneous and rapid cooling in the cavity as the material vitrifies, and they often lead to complex residual stress and birefringence patterns [15–17]. For a one-dimensional case of a simple vitrifying liquid, the cooling stress can be scaled as

$$\sigma_c \sim \alpha \left(T_g - T_{mold}\right) \frac{EH^2}{(1-\nu)}. \tag{1.5}$$

Where α is the thermal expansion coefficient, E is Young's modulus, ν is Poisson's ratio of the solid polymer, and H is a characteristic thickness of the molded article. It must be noted that although Eq. 1.5 applies specifically to the case of free quenching of a slab, quite unlike the quenching in an enclosed molding cavity (constrained quenching) [18,19], it may be used for scaling purposes. Based on Eq. 1.5, we can define a characteristic surface distortion (strain) by

$$\delta_c \sim \alpha \left(T_g - T_{mold}\right) H^2 \tag{1.6}$$

Thus, the distortion induced by cooling stresses can be minimized by raising the mold temperature closer to T_g and by reducing the thickness of the part. In general, however, the residual stress distribution in the molding cavity is determined not only by thermal shrinkage but also by differential compression of the polymer melt during vitrification inside the cavity. Thus, tensile residual stresses are typically produced at the cavity surfaces wherein the material vitrifies under relatively low pressures during the filling phase, while compressive residual stresses are present away from the surfaces where vitrification occurs under relatively high pressures during the packing stage. The resulting residual stress can be superimposed on the thermal stresses represented by Eq. 1.5. At high mold temperatures the relative contribution of thermal stresses becomes small (see Eq. 1.6) and the pressure-induced residual stresses dominate. The presence of high residual tensile stresses at the surfaces of the part may lead to part failure, e.g., by crazing.

1.3.3 Shrinkage

The "shrinkage" (i.e., the change in volume of the molded article as it cools down freely after ejection from the mold) can be viewed as a manifestation of volume contraction associated with the change in temperature as the part cools from its terminal temperature immediately after t_e(T_e^+ at t_e^+) to ambient. If one employs long cooling times, i.e., the material is allowed to thermally equilibrate inside the cavity (as recommended for PIM operations, see above), the temperature of the part is approximately uniform and equal to T_{mold} at t_e, and the total volume contraction can be estimated from

$$\Delta v \sim 3\alpha \left(T_{mold} - T_{amb}\right) v_o \tag{1.7}$$

The corresponding linear contraction strain is

$$\delta_s \sim \alpha \left(T_{mold} - T_{amb}\right) \tag{1.8}$$

Thus, the shrinkage will be small if T_{mold} is close to T_{amb}. However, because of detrimental effects on replication fidelity and cooling stress (Eq. 1.5) it is desirable to select T_{mold} closer to T_g and well above T_{amb}. For a finite residual pressure (P_r) at t_e the observed shrinkage is

partially offset by the decompression of the material as the part is ejected from the mold, and the pressure drops abruptly to ambient (Fig. 1.3).

1.3.4 Warpage

If the cooling to T_{amb} is uniform, the only effect of shrinkage is an absolute change in dimensions relative to the dimensions of the mold cavity, which can be readily compensated through changes in mold design. In most cases, however, the shrinkage is not uniform because of the flow-induced anisotropy of the thermal expansion coefficient and the spatial nonuniformity of the thermo-mechanical history and the corresponding residual stresses in the cavity. This nonuniformity can lead to "warpage," i.e., a shape distortion, in addition to volumetric contraction, which can be characterized by the following distortion strain (assuming it is dominated by the anisotropy of the thermal expansion coefficient),

$$\delta_w \sim f\left(\alpha\| - \alpha\perp\right)\left(T_g - T_{amb}\right) \tag{1.9}$$

where $\alpha\|$ and $\alpha\perp$ are the values of the thermal expansion coefficient parallel and perpendicular to the polymer chain axis, and f is a spatially variable orientation function ($-0.5 \leq f \leq 1$) representing the "frozen-in" molecular orientation in the solid part. The higher the anisotropy of the polymer matrix, the higher the absolute magnitude of f, and the higher the potential warpage of the molded article. Another potential cause for warpage is nonuniform mold temperature. If, for example, the two mold halves are not thermally balanced, a temperature gradient and a corresponding thermal stress will ensue across the part at t_e. As the mold opens, this thermal stress is relieved causing the ejected part to warp as soon as the temperature of the part approaches T_{amb} [20, 21]. This underscores the need to control and maintain uniform temperature in precision molds through improved design and maintenance of the mold cooling/heating system and better temperature control algorithms. More complete discussions of the shrinkage and warpage problems in injection molding can be found in chapters 3 and 5 of this volume [14, 22].

1.4 Dimensional Stability

By *dimensional stability* we mean the ability of the part to maintain its configuration within the specification range over time. The dimensional stability of the part is influenced by several external and internal factors including: (a) adverse environmental conditions (e.g., exposure to varying temperature and humidity), (b) physical aging, (c) recovery of internal residual strains, and (d) viscoelastic effects in response to external stresses (e.g., stress relaxation and creep). The relative importance of these factors depends on the physical properties of the solid polymer, the levels of residual stress and anisotropy in the molded part, and the prevailing environmental conditions during the useful lifetime of the article. If the part is not subjected to large external stresses during its functional use, moisture absorption, temperature fluctuations, physical

aging, and relaxation of internal stresses are the major mechanisms driving dimensional instability.

Physical aging (or volume recovery), usually manifested by a spontaneous rise in density, is inherently present in any glassy polymer [23]. For kinetic reasons the polymer cannot reach thermodynamic equilibrium as it is cooled through the glass transition. Consequently, an excess free volume is built up in the material, which will decrease slowly over time. Struik has shown that the kinetics of the aging process far from equilibrium can be represented by a characteristic "rate" parameter [23]:

$$\beta \equiv -\frac{1}{v}\,\frac{\partial v}{\partial \log t_a} \tag{1.10}$$

where v is the specific volume, t_a is the aging time, and β is a material characteristic that depends on temperature and the molecular structure of the polymer. This relationship has been explained in terms of the self-retarding nature of physical aging, i.e., with increasing density the molecular mobility of the material is reduced, and the aging process becomes increasingly more sluggish. Wimberger-Friedl and de Bruin have shown that the semi-logarithmic aging kinetics expressed by Eq. 1.10 does not hold for very long aging times in the case of polycarbonate, a polymer frequently used in high precision applications. For this material, a strong increase in the slope of the volume contraction curve on a logarithmic time scale (apparent β) was observed during aging at room temperature [24]. The temperature dependence of β for several amorphous polymers is illustrated in Fig. 1.4. For polymers with "weak" sub-T_g relaxations, the temperature dependence of β below T_g can be scaled by

$$\beta \sim \exp\left(T - T_g\right) \tag{1.11}$$

Thus, the rate of aging increases exponentially as the use temperature approaches T_g. This clearly suggests that high-T_g polymers with weak secondary relaxations are less susceptible to aging-induced dimensional changes due to the slower rate of aging at ambient conditions.

The volume recovery of polymers in the glassy state can also be influenced by pressure applied during vitrification (formation pressure), which may directly impact the density and dimensional stability of a molded article. When vitrified under pressure, the density of an amorphous polymer at ambient conditions is generally increased through an effect known as pseudo-compressibility [25]. The dependence of density on the formation pressure typically leads to density nonuniformity within the molded part [13, 26, 27] and may have a detrimental effect on its dimensional stability. During volume recovery the material formed under pressure tends to expand over time, thus offsetting to some extent the contraction associated with physical aging [27].

The aging rate can be reduced not only by the proper choice of material but also by a judicious annealing treatment. It has been noted [28] that the most efficient annealing occurs at $\sim$ 10–20 °C below T_g, rather than at or near T_g, since by annealing close to T_g the glassy polymer is actually "rejuvenated" and the reduction in β is smaller. A judicious annealing program can be readily combined with the injection molding cycle; by proper selection of T_{mold} and the residence time in the mold (t_e), the thermal equilibration portion of the cooling stage ($t_{cool} < t < t_{cure}$, see Fig. 1.1) may overlap with the annealing step.

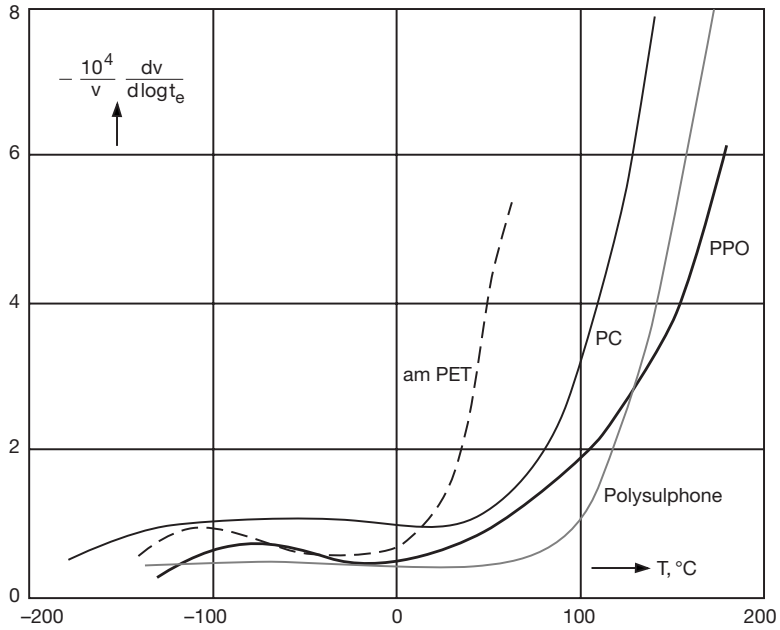

Figure 1.4: Aging rate parameter (β) vs. temperature for several amorphous polymers [28] (Reproduced with permission of J. Wiley, Ltd.)

It has been shown that residual orientation stresses (stresses generated above T_g during the filling and packing stages, see Fig. 1.2) can give rise to an accelerated anisotropic shrinkage. This shrinkage is equivalent to the viscoelastic creep recovery effect, and it can be estimated from linear viscoelasticity theory by [28]

$$\delta_R \sim \sigma_R J\,(T_{amb}, t) \tag{1.12}$$

where δ_R is the recovery strain associated with a residual orientation stress, σ_R, which is the effective stress applied at the instant of vitrification, and J is the creep compliance of the material at ambient conditions. It is, thus, seen that the spontaneous deformation of the molded part can be minimized by lowering the level of residual stress in the part and/or by selecting materials with low compliance under ambient conditions. As noted above, lower residual stress is also desirable for minimizing warpage strain (Eq. 1.9). From careful measurements of the anisotropic dimensional changes of injection molded parts, Schennink has shown that at temperatures far below T_g the shrinkage is isotropic, thus indicating that physical aging is the dominant effect at low temperatures, while at elevated temperatures anistropic shrinkage is the prevailing effect [29]. General approaches for minimizing residual stress (and birefringence) in injection molded parts have been discussed elsewhere [30]. In cases involving relatively low internal stresses (e.g., various optical components having low birefringence), physical aging is likely the dominant factor controlling the dimensional stability of the part (chapter 7 [31]).

HANSER

Precision Injection Molding

Jehuda Greener, Reinhold Wimberger-Friedl

Process, Materials and Applications

ISBN 3-446-21670-7

8 Injection Molding for Microfluidics Applications

L. J. Lee, L. Yu, K. W. Koelling, and M. J. Madou

8.1 Introduction

Miniaturization methods and materials are well developed in the integrated circuit industry. They have been used to produce a variety of commercial microdevices, such as camera and watch components, printer heads, automotive sensors, microheat exchangers, micropumps, microreactors, etc., in the last 15 years [1, 2]. This new field is known as microelectromechanical systems (MEMS), with a combined international market size of over $15 billion in 1998 [3]. In recent years MEMS applications have also been extended to optical communication and biomedical fields. The former is called micro-optic-electromechanical systems (MOEMS), while the latter is known as bio-microelectromechanical systems (BioMEMS). Potential MOEMS structures include optical switches, connectors, grids, diffraction gratings, and miniature lenses and mirrors. Potential and existing BioMEMS products are biochips/sensors, drug delivery systems, advanced tissue scaffolds, and miniature bioreactors.

Current microdevices are largely based on silicon (Si), owing to extensive development of microfabrication methods (e.g., lithography, thin film deposition, wet/dry etching) by the microelectronics industry. Unfortunately, the physical and chemical properties of Si-based materials (poor impact strength/toughness, lack of optical clarity, and poor biocompatibility) are not appropriate for many applications. For example, the conductivity of silicon is problematic in many BioMEMS applications that require high voltage for electrokinetic flows. Nonconductive glass or quartz microdevices can be made using the same lithography/etching fabrication techniques. These materials, although less costly than silicon, are still much more expensive than most polymeric materials [4]. In contrast, many polymers exhibit high toughness, optical clarity, and recyclability. Some also possess excellent biocompatibility and can provide various biofunctionalities. Future markets for biomedical microdevices for the human genome, drug discovery, and delivery in the pharmaceutical industry, clinical diagnostics, and analytical chemistry are enormous (tens of billions of US dollars [5]).

Microscale fabrication methods of polymeric materials have been explored in recent years both in industry and in academia [4, 6]. Although large-volume production is still rare, many manufacturing processes and commercial machines are available in the market. The major challenge now is to modify these processes and to optimize the processing conditions such that low-cost, high-speed, and high-quality mass production can be realized as in the macroscale production.

Of the available techniques in plastic molding, injection molding is the most commonly used. It has the advantages of good dimensional control, a short cycle time, and high productivity. The term microinjection molding refers to making either microscale parts or parts with microscale features. For the former, the delivery system, such as the runner and the sprue, is often much larger compared to the microparts. For the latter, the part itself contains features in very different size scales. Therefore, microinjection molding always faces flow and heat transfer through multiscale structures. In this chapter, injection molding of regular-sized parts with microfeatures is considered with primary interest on microfluidic devices. Injection molding for micron-sized parts is discussed in a separate chapter. We first introduce the basic microfluidic concepts and important microfluidic functions (section 8.2). Various mold-making methods at the microscale will then be described (section 8.3) with a focus on X-ray LIGA and UV-LIGA processes because of their wide applications in making microfluidic devices. This is followed with a brief survey on various microfeature injection molding methods and applications (section 8.4). Since CDs and DVDs are the most well-known injection molding products containing microscale features, their manufacturing processes will be presented first. Finally, experimental and theoretical analyses of injection molding with microfeatures are discussed (sections 8.5 and 8.6). The chapter ends with a short conclusion including suggested future research and development directions (section 8.7).

8.2 Microfluidics

8.2.1 Basic Concepts

Microfluidics is the manipulation of fluids in channels, with at least two dimensions at the micron or sub-micron scale. If the channel dimensions are less than 100 nanometers, the fluid flow is referred to as nanofluidics. This is a core technology in a number of miniaturized systems developed for mechanical, chemical, biological, and medical applications. Although both gases and liquids are used in micro- and nanofluidic applications [7, 8], the low-Reynolds-number hydrodynamics covers most microfluidic applications. Typical Reynolds numbers for fluids flowing in microchannels with linear velocities in the range up to 10 cm/s are less than 30 [9]. Therefore, viscous forces dominate the response and the flow remains laminar.

Fluid motions in these small-scale systems can be driven by either applied pressure difference, electric fields associated with charged Debye double layers (or electrical double layer-EDL) common when ionic solutions are present, or capillary driving forces owing to wetting of surfaces by the fluid [9]. The pressure-driven flow is similar to the classic Poiseuille flow. The electrokinetic effects can result in either electro-osmotic flow (EOF) or electrophoretic responses. EOF is a bulk flow motion driven by stresses induced in the thin EDL (i.e., 1 to 10 nm) near the channel walls, caused by an imposed electric field across the channel length. The velocity profile in the core of the channel is mostly plug-like, even for a channel height as small as 24 nm [10]. Higher electrical permittivity of the fluid, imposed electric field strength, and zeta potential on the wall surface may all increase the flow rate. Electrophoretic response, on the other hand, is the motion of charged molecules in a fluid caused by an

electric field imposed across the channel length. The positively charged molecules move to the negative electrode, while the negatively charged molecules move towards the positive electrode, leading to molecular separations. This electrophoresis technique is the most widely used separation method in the biotech field today. Typically, a buffer solution is chosen such that all biomolecules in the fluids, e.g., DNA/RNA fragments and proteins, are negatively charged. They will all migrate from the sampling point to the detection point. Since DNA molecules have uniform charge-mass ratios regardless of their length, separation is usually achieved by placing an immobilized gel or a mobile *gel* or *sieving* solution in the separation channel [11–13]. EOF may cause unwanted washout of the gel solution during electrophoresis, so a functional channel coating may be necessary for EOF suppression if the channel wall contains a high zeta potential (e.g., glass) [13]. On the other hand, undesirable electrophoretic separation may occur in EOF if the sample solution contains components with different charges. A high-ionic-strength-plugs method was developed to facilitate sample transport [11]. The use of solutions at different ionic strengths and therefore different electroosmotic mobility, however, creates a quite complex situation in microfluidics. The electrokinetic flow works very well in microchannels because of the large surface-to-volume ratio, which minimizes the Joule heating problem in this type of flow. Very high electric field strength (i.e., hundreds to thousands of volts per centimeter of channel length) can be easily applied in microdevices to speed up the processing time, from hours to minutes or even seconds [11]. For nano-sized channels, it has been found that very low electric power (e.g., several volts per micron channel length) can generate a volume flow rate that is practical for controlled drug delivery [10].

Capillary forces are also highly favorable in microfluidics. This method is simple and low-cost, but a gas–liquid interface must exist. The velocity profile is similar to that in the pressure-driven flow, but the flow is very sensitive to the surface tension of the fluid, the solid surface energy and roughness, and the channel shape [14]. Active control of surface tension forces to manipulate flows in microchannels can be achieved by forming gradients in interfacial tension on the channel surface [15] or electrowetting [16].

For most cases involving the flow of small molecule liquids like buffer solutions, the standard continuum description of transport processes works very well, except that surface forces (surface tension, electrical effects, van der Waals interactions, and in some cases steric effects) play a more important role than usual. Although some discrepancies have been reported between pressure-driven flow measurements made in microchannels and calculations based on the Navier-Stokes equations, most have been found to be experimental errors [9]. This is because the pressure drop as a function of flow rate varies as the inverse fourth power of the radius (or inverse third power of channel height), and a small change in the radius (or channel height) due to manufacturing imperfections or channel-wall contamination produces large changes in the flow. Since the volumetric flow rate varies linearly with channel radius (or height) for electrically driven flow, EOF is a more reliable way to verify microfluidic experiments with calculations. A recent study [10] shows that calculated flow rates from the classical EOF analysis agree well with experimental data for channel heights in the range of 10 to 20 nm.

Retardation of ionic liquids and solutions in microchannels, however, can be significant when the channel walls contain either the same static charge [17] (e.g., glass surface is negatively charged) in the pressure-driven flow or opposite charges in EOF [10]. In the former case, the flow causes charges inside the EDL to accumulate downstream, while charges on the solid

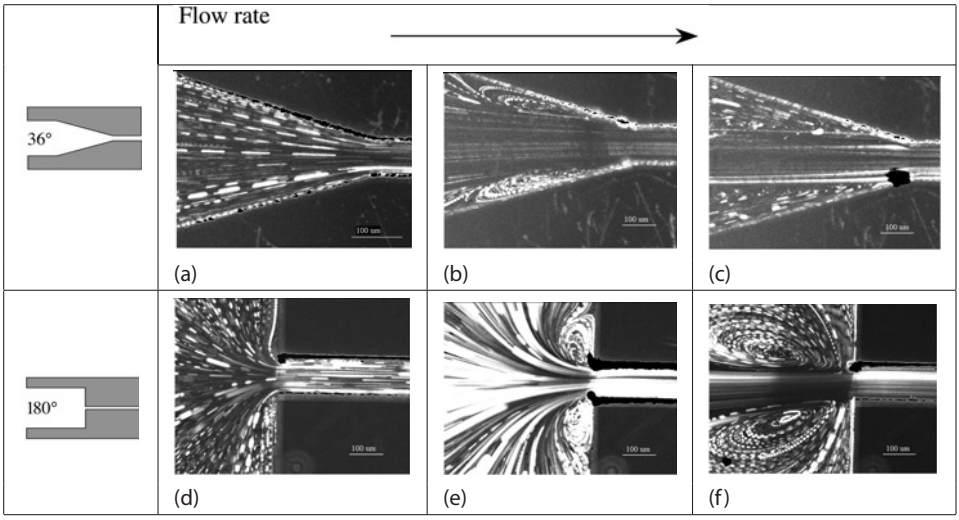

Figure 8.1: Streak photograph of the entrance flows –vortex enhancement (ext strain = 6.36. Material: 2 % wt PEO Mv = 4,000,000)
(a) Triangular ends: shear rate = $5.9 \times 10^2\ s^{-1}$, shear stress = 1.0×10^2 Pa, Re = 6.3×10^{-3}, Wi = 20.1, average extensional rate = $0.57\ s^{-1}$
(b) Triangular ends: shear rate = $1.8 \times 10^3\ s^{-1}$, shear stress = 1.7×10^2 Pa, Re = 6.1×10^{-2}, Wi = 42.5, average extensional rate = $2.9\ s^{-1}$
(c) Triangular ends: shear rate = $4.5 \times 10^3\ s^{-1}$, shear stress = 2.5×10^2 Pa, Re = 3.0×10^{-1}, Wi = 78.9, average extensional rate = $8.6\ s^{-1}$
(d) Flat ends: shear rate = $4.5 \times 10^2\ s^{-1}$, shear stress = 8.0×10^1, Re = 3.2×10^{-3}, Wi = 16.7
(e) Flat ends: shear rate = $1.5 \times 10^3\ s^{-1}$, shear stress = 1.4×10^2, Re = 2.9×10^{-2}, Wi = 37.6
(f) Flat ends: shear rate = $2.6 \times 10^3\ s^{-1}$, shear stress = 1.9×10^2, Re = 7.8×10^{-2}, Wi = 54.5

channel wall remain immobile. Such excess charge creates a potential drop in the channel direction that causes a "back flow." For channel heights in the range of 100 microns, this electroviscous effect (flow retardation is often counted as an increase in fluid viscosity) is small. But a retardation of 70 % is observed when the glass channel diameter is in the range of several microns [17]. In the latter case, the back flow can be manipulated by surface micropatterning of opposite charges on the walls of a microchannel to achieve laminar chaotic mixing [18] or controllable membrane permeation.

In microchannels, the shear rate can be very high, e.g., $10^7\ s^{-1}$, even though the Reynolds number is low. Rheological characterization of polymeric fluids and biofluids in such a flow field has recently been studied in our laboratory [14]. It was found that the standard rheological analysis used at the macroscale can also be applied to characterization at the microscale. For solutions containing high molecular weight polymer (or DNA) molecules, polymer degradation is substantial when the shear stress and shear rate are high.

Vortex enhancement has been observed in "extension-thickening" solutions (e.g., high molecular weight polyethylene oxide (PEO) in water) flowing in microscale contractions and expansions. At low flow rates, the flow is a perfect laminar flow (Figs. 8.1a and d). Small vortices

emerge at increased flow rate (Fig. 8.1b and e). Figures 8.1(c and f) show the growth of vortices with flow rate (vortex enhancement). Clearly, this trend is contrary to the observation of Newtonian fluids, where vortices decrease in size with the increasing flow rate or Reynolds number. Vortex enhancement is strongly effected by the fluid elasticity. However it does not occur in all viscoelastic materials.

The rheology of polymer melts and solutions flowing in microchannels and micromolds needs further study because many polymers exhibit strong non-Newtonian and viscoelastic behavior in these extremely thin and confined flows.

8.2.2 Micro- and Nanofluidic Functions

A wide range of microfluidic functions, such as pumps, valves, mixers, and flow sensors, has been demonstrated [7–9, 19–21]. The main challenge in making miniaturized systems is the integration of different microfluidic functions to perform a certain analysis at high speed and high throughput. Integrated microfluidic systems have the potential for microheat transfer, microreaction technology, bioseparation, clinical diagnostics, drug discovery and delivery, and lab-on-a-chip technology. Most microfluidic systems are built on silicon, glass, or rigid polymer substrates. For prototyping, rubbery polymers like polydimethylsiloxane (PDMS) made from the simple casting process can be used. Quake and his coworkers [21] have fabricated elastomeric microfluidic devices for cell sorting and biochemical assays.

Various microfluidic propulsion technologies have been reviewed and compared by Madou et al. [19, 22] with regard to the choice of materials, the maturity of the technology, and the achievable volumetric flow rates. In general the fluid propulsion can be generated mechanically, electrically, or thermally. In the pressure-based approach, a mechanical pump is often used to provide the driving pressure. The pump can be as simple as a roller in the blister pouch design [23] or as complicated as a miniaturized syringe or acoustic pump [24]. The former is simple, low-cost, and readily available; however, it has little opportunity for further miniaturization or for high throughput tests. The latter is costly and the choice of materials is limited to piezoelectrics for acoustic pumping. Pressure-based propulsion does have the attractive feature of being generic for pumpable fluids.

On the other hand, electrokinetic techniques such as electro-osmosis or electrophoresis, electrodynamics, and electrowetting have the advantage that they scale favorably for miniaturization. In electro-osmosis or electrophoresis, the driving forces for flow are generated by the interaction of applied electric fields with ionic species in the fluids. In electrodynamics, the flow is generated by the interaction of electric fields with induced electric charges in the fluids. Electrowetting is based on the principle that the contact angle between a liquid and a solid surface can be changed through the application of an electrical potential [16]. This change may result in capillary forces that provide a driving pressure in a small flow channel. Since these techniques become more effective with decreasing volume size and increasing surface area, they are very attractive in microfluidic applications. However, they need high electric fields and depend strongly on the properties of fluids to be pumped (such as pH or charges). Many organic compounds and solvents may not be able to meet the charge and pH requirements. Thermal methods can also be used for fluid propulsion. Sammarco and Burns [25]

manipulated the contact angle between a liquid and a solid surface by changing the local fluid temperature. The resulting capillary force is used to drive the fluid as in electrowetting. In the case of phase-change pumping [29], the driving pressure arises from the volume change due to the phase change from liquid to gas, as the liquid is heated. Considering the high heat exchange rate in small channels, this mechanism scales well down to the microdomain. Thermal methods are still in the early research stage and they require careful control of the local temperature.

By contrast, in centrifugal pumping, fluid propulsion is achieved through rotationally induced hydrostatic pressure. It is simple, uses a single low-cost motor, and is capable of fine flow control through proper design of the location, dimensions, and geometry of channels and reservoirs based on fluid properties. It can also be easily integrated with the information-carrying capacity of the CD [19].

Another essential component in the microfluidic system is the ability to stop and start the fluid flow. Conventional diaphragm valves [25, 27–29] can fulfill this task, but they usually require moving parts and an external actuation mechanism, such as a change in temperature, pH, or charge. Controlling the liquid flow electrokinetically has been widely used for DNA sequencing. This method, however, requires a high electric field, is sensitive to the properties of the fluids, and may lead to the occurrence of Joule heating. An alternative approach is to use a passive capillary-valve that relies on the capillary force to stop the flow in microchannels. The principle of operation is based on a pressure barrier that develops when the cross section of the capillary expands abruptly. Capillary valving has the advantage of not requiring any moving parts and external actuation. Recently this type of valve has attracted a great deal of attention and has a strong appeal for applications in various microfluidic systems [19, 22].

Because of the micron-sized flow channels, the Reynolds number of fluid flow in the microfluidic systems is extremely small (usually less than 1). The lack of turbulent flow makes the mixing in microdevices a very challenging issue. Diffusion is the main driving force in micromixing due to the nature of laminar flow. Design of micromixers is generally based on increasing the diffusion time, enlarging the contact area, and creating more chaotic flows.

The enlargement of the contact surface between two fluids can be achieved in many different ways. Static-type (i.e., no moving parts) micromixers based on the concept of lamination [30, 31] or separation-reunification [32] have been developed and studied. A similar approach is to divide each flow into several partial flows in order to increase the contact area. Injecting one liquid into another liquid with microplumes can achieve the same goal [31]. The basic principle of these micromixers is to decrease the diffusion length required for mixing. Some of the static micromixer designs can be complicated, e.g., the lamination type where very precise alignment is required [33].

A chaotic flow field can be generated with two pumps connected via source and sink to a mixing chamber [34]. This design employs chaotic advection for mixing. It is more efficient than static mixers, but it requires expensive instrumentation. In electrokinetic-based microfluidic systems, convective mixing can be achieved by inducing surface charges at the interface of liquid samples that have different conductivities. The surface charges react with the applied electric fields to generate electric shear forces. The separate flow streams mix when passing the electrodes. Successful mixing results have been demonstrated [35]. One can also place a solid post in the middle of the microflow channel. By applying one electric field to the surface

of the channel wall and an opposite electric field to the surface of the post, convective mixing can be achieved when the fluids pass the post. Surface micropatterning of opposite charges on the walls of a microchannel can also achieve laminar chaotic mixing [18]. However, this kind of mixing depends on the physiochemical properties of fluids and, therefore, is limited in its application.

Delivery of precisely metered fluids from one reservoir to another in a well-controlled sequence is important in many microfluidic applications. Several methods have been developed for this purpose. An on-chip technique to meter discrete nanoliter-sized liquid drops inside microchannels was developed, using a combination of a hydrophobic surface treatment and air pressure [36]. This technique involves spontaneously filling the microchannel up to a hydrophobic stop and splitting a liquid drop by injecting air through a hydrophobic side channel. Accurate liquid volumes, ranging from 0.5 to 125 nl, were metered using this technique. Another method is to draw a liquid sample from a larger reservoir to a number of smaller capillaries and let the excess liquid flow into an overflow chamber. The capillaries containing metered liquid samples can then be released in sequential order by capillary valving as described in flow sequencing [25]. These methods, however, require fairly complicated design and implementation.

The flow of fluids through nanochannels may bring many functional components for microfluidic biomedical diagnostic systems, as well as control of the transport of biomolecules for drug delivery applications. This is due to the increasing ionic concentration within the nanochannels with decreasing channel height (resulting from electrochemical effects) and the increase in voltage drop across the membrane for decreasing channel height (resulting from far-field voltage and resistance effects) [10]. Future research in this area will deal with molecular transport within these nanochannels and the design of tailored electrolytes for specific micro- and nanofluidic systems. Actively controlled permeable/impermeable membranes/biocapsules for bioseparation, immunoprotection, and drug delivery can be achieved.

8.3 Mold (Master) Making

The mold inserts (or masters) can be fabricated by a variety of techniques. For large features ($> 50\,\mu m$) with tolerances and repeatability in the range of about $10\,\mu m$, traditional computer numerically controlled (CNC)-machining and wire electrodischarge machining (EDM) of materials like tool steel and stainless steel are often accurate enough. The advantage of this technique is that the tool materials used are the same as those in conventional polymer molding, so their design, strength, and service life are well established. Complicated 3-D structures can also be machined easily. The main drawbacks are that it is difficult to make sharp corners or right angles, and the surface quality is usually poor (surface roughness around several μm) [37]. Diamond-based micromilling/microdrilling [38], micro-EDM, and excimer or femtosecond laser-based [39] direct removal processes can reduce the surface roughness to $1\,\mu m$ or less [40]. While diamond-based methods can also make features smaller than $10\,\mu m$, they are only applicable to "soft" metals such as nickel, aluminum, and copper. For prototyping, most of these methods can be directly used on polymeric materials to fabricate

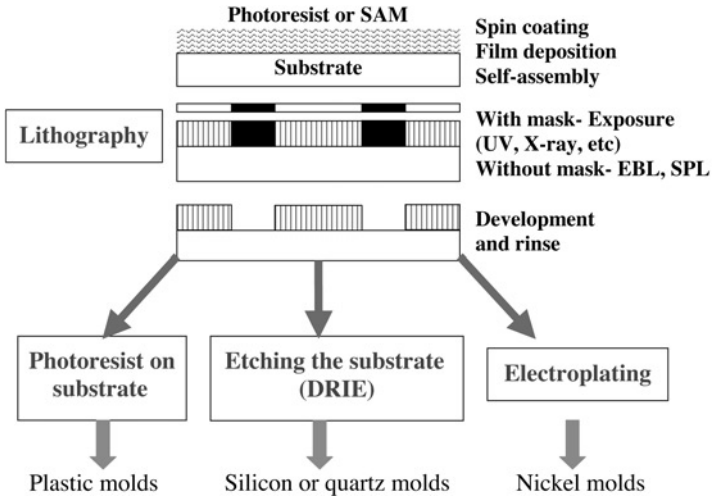

Figure 8.2: Schematic of surface machining methods of a master

microfluidic devices. For smaller feature sizes (down to one micron or less), photolithographic methods, e-beam lithography (EBL), or scanning probe lithography (SPL, such as AFM dip pen lithography [41, 42]) have to be employed (i.e., surface machining). Here, a liquid photoresist or self-assembled monolayer (SAM) is placed on a galvanic starting layer by either spin-coating, thin film deposition or self-assembly. The microfeatures are formed after either radiation exposure through a photomask and development or direct e-beam or scanning probe writing. Figure 8.2 shows a schematic of these surface machining methods. For prototyping, this photoresist structure can serve as a microdevice itself or be used as a mold (called photoresist mold) in low temperature and low-pressure molding processes. More generally, this structure is either used directly for electroplating or for wet/dry etching of silicon, which is subsequently electroplated [1]. Both technologies yield a metal tool, usually nickel or nickel-cobalt. For features with a low aspect ratio (defined as the ratio of feature depth to width) or for rapid prototyping where the lifetime of mold inserts is not crucial, a glass or silicon wafer etched by wet or reactive-ion etching (RIE) can be utilized directly as a mold insert. For very small features ($< 1\,\mu m$) with high aspect ratios (up to 100 or higher), technologies like LIGA [1, 43] in thick resists (like EPON SU-8) or Deep RIE (DRIE) are needed to obtain the mold insert.

8.3.1 LIGA

LIGA is the German acronym for X-ray lithography (Roentgen Lithographie), electrodeposition (Galvanoformung), and molding (Abformtechnik). The process involves a thick layer of X-ray resist coated on a substrate (from microns to centimeters) followed by high-energy X-ray radiation exposure and development to arrive at a three-dimensional resist structure. Subsequent metal deposition fills the resist mold with a metal and, after resist removal, a

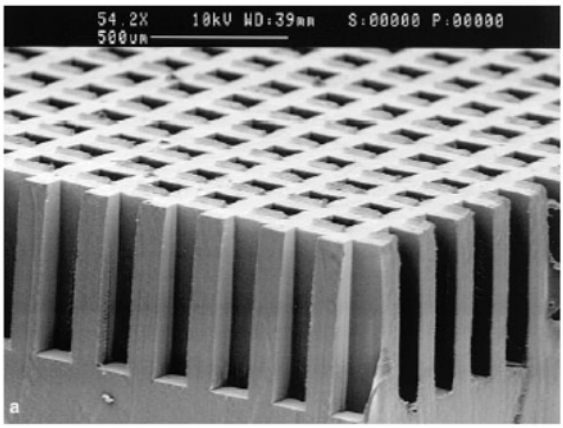

Figure 8.3: SEM micrograph of HDPE molded microstructure [44, with permission]

freestanding metal structure results [43]. The metal shape may serve as a mold insert for precision injection molding at the microscale. The plastic mold retains the same shape, size, and form as the original resist structure but is produced quickly and inexpensively as part of an infinite loop. Figure 8.3 shows a SEM micrograph of a high-density polyethylene (HDPE) microstructure molded by Despa et al. [44].

The bandwidth of possible sizes in all three dimensions renders LIGA useful for manufacture of microstructures (micron and submicron dimensions), of packages for these microstructures (millimeter and centimeter dimensions), and even for the connectors from those packages to the "macro world" (electrical, e.g., through-vias or physical, e.g., fluid in- and outlets).

Romankiw and coworkers at IBM first carried out combining electrodeposition and X-ray lithography as early as 1975 [45]. These authors made high-aspect-ratio metal structures by plating gold in X-ray–defined resist patterns of up to 20 µm thick. They had, in other words, already invented "LIG"; that is, LIGA without the *Abformung* (molding). This IBM work was an extension of through-mask plating, also pioneered by Romankiw et al. in 1969, and was geared toward the fabrication of thin film magnetic recording heads [46]. The addition of plastic molding to the lithography and plating process was realized by Ehrfeld et al. [47] at the Kernforschungszentrum Karlsruhe, or KfK, in 1982. By adding molding these pioneers recognized the broader implications of LIGA as a new means of low-cost manufacturing of a wide variety of microparts with unprecedented accuracies from various materials previously impossible to batch fabricate [47]. In Germany, LIGA originally developed almost completely outside of the semiconductor industry. In the United States, it was the late Henry Guckel, who, starting in 1988, repositioned the field in light of semiconductor process capabilities and brought it closer to standard manufacturing processes [48].

Today the construction cost for a typical synchrotron totals over $30 million, restricting the access to LIGA. Obviously one would like to find less expensive alternatives for generating intense X-rays [49]. Currently, there are a number of synchrotron facilities worldwide that have beam lines dedicated to micromachining work [51–54].

X-ray Mask

X-ray mask production is one of the most difficult aspects of X-ray lithography. For highly transmissive materials, the mask substrate for X-rays by necessity must be a low Z (atomic number) thin membrane. X-ray masks should withstand many exposures without distortion, be alignable with respect to the sample, and be rugged. The requirements for X-ray masks in LIGA differ substantially from those for the IC industry [55]. The main difference lies in the absorber thickness. To achieve a high contrast (> 200), very thick absorbers (> 10 µm vs. 1 µm) and highly transparent mask blanks (transparency > 80 %) must be used because of the low resist sensitivity and the great depth of the resist. Another difference focuses on the radiation stability of membrane and absorber. For conventional optical lithography, the supporting substrate is a relatively thick, optically flat piece of glass or quartz highly transparent to optical wavelengths. It provides a highly stable (> 10^6 µm) basis for the thin (0.1 µm) chrome absorber pattern. In contrast, the X-ray mask consists of a very thin membrane (2 to 4 µm) of low-Z material carrying a high-Z thick absorber pattern [56]. A single exposure in LIGA results in an exposure dose a hundred times higher than in the IC case.

Due to excellent contrast and good process stability of e-beam lithography (a process often used to produce X-ray masks), PMMA is the preferred resist for deep-etch synchrotron radiation lithography. Two major concerns with PMMA as a LIGA resist are a rather low lithographic sensitivity and a susceptibility to stress cracking. To make throughput for deep-etch lithography more acceptable to industry, several avenues to more sensitive X-ray resists have been pursued. For example, copolymers of PMMA were investigated: methyl methacrylate combined with methacrylates with longer ester side chains show sensitivity increases of up to 32 % (with tertiary butylmethacrylate). Unfortunately, deterioration in structure quality was observed [57]. Among the other possible approaches for making PMMA more X-ray sensitive, we can count on the incorporation of X-ray absorbing high-atomic-number atoms or the use of chemically amplified photoresists. X-ray resists explored more recently for LIGA applications are polylactides, for example, poly(lactide-co-glycolide) (PLG), polymethacrylimide (PMI), polyoxymethylene (POM), and polyalkensulfone (PAS). PLG is a new positive resist developed by BASF AG, more sensitive to X-rays by a factor of 2 to 3 compared with PMMA. Its processing is less critical. From the comparison of different resists for deep X-ray lithography, PLG emerges as the most promising LIGA resist. POM, a promising mechanical material, may also be suited for medical applications given its biocompatability. All of the resists exhibit significantly enhanced sensitivity compared to PMMA, and most exhibit a reduced stress corrosion [58]. Negative X-ray resists have inherently higher sensitivities compared to positive X-ray resists, although their resolution is limited by swelling. Poly(glycidyl methacrylate-co-ethyl acrylate) (PGMA), a negative e-beam resist, has also been used in X-ray lithography. In general, resist materials sensitive to e-beam exposure also display sensitivity to X-rays and function in the same fashion; materials positive in tone for e-beam radiation typically are also positive in tone for X-ray radiation. A strong correlation exists between the resist sensitivities observed with these two radiation sources, suggesting that the reaction mechanisms might be similar for both types of irradiation. Different methods to apply ultrathick layers of PMMA have been studied. In the case of multilayer spin coating, high interfacial stresses between the layers can lead to extensive crack propagation upon developing the exposed resist.

Adhesion promotion by mechanically or chemically modifying the primary substrate is important. Smooth surfaces such as Si wafers with an average roughness, R_a, smaller than 20 nm pose additional adhesion challenges often solved by modifying the resist itself. To promote adhesion of the resist to polished untreated surfaces, such as metal-coated Si wafers, coupling agents must be used to chemically attach the resist to the substrate. An example of such a coupling agent is methacryloxypropyl trimethoxy silane (MEMO). With 1 wt % of MEMO added to the casting resin, excellent adhesion results. The adherence is brought about by a siloxane bond between the silane and the hydrolyzed oxide layer of the metal. Hydroxyethyl methacrylate (HEMA) can improve PMMA adhesion to smooth surfaces but higher concentrations are needed to obtain the same adhesion improvement. Silanization of polished surfaces prior to PMMA casting, instead of adding adhesion promoters to the resin, did not seem to improve the PMMA adhesion at the base.

For many applications stepped or inclined resist sidewalls are very useful (i.e., the fabrication of multilevel devices or prisms or, more basic yet, angled resist walls to facilitate the release of molded parts). To make good resolved stepped features one can first relief print a PMMA layer, for example, by using a nickel mold insert made from a first X-ray mask. Subsequently, the relief structure may be exposed to synchrotron radiation to further pattern the polymer layer through a precisely adjusted second X-ray mask. To carry out this process, a two-layer resist system needs to be developed consisting of a top PMMA layer which fulfills the requirement of the relief printing process, and a bottom layer which fulfills the requirements of the X-ray lithography [59]. The bottom resist layer promotes high molecular weight and adhesion, while the top PMMA layer is of lower molecular weight and contains an internal mold-release agent. The two-step resist then facilitates the fabrication of a mold insert by electroforming, which can be used for the molding of two-step plastic structures. Extremely large structural heights can be obtained from the additive nature of the individual microstructure levels.

To achieve miniaturized features with slanted walls one has several options. One can modulate the exposure/development times of the resist, fabricate an inclined absorber, angle the radiation, or move the mask during exposure in so-called moving mask deep X-ray lithography (M^2DXL). To make a slanted absorber one can etch a slab of material into a wedge by pulling it at a linear rate out of an etchant bath. Changing the angle at which synchrotron radiation is incident upon the resist, usually 90°, also enables the fabrication of microstructures with inclined sidewalls [60]. This way slanted microstructures may be produced by a single oblique irradiation or by a swivel irradiation. One potentially very important application of microstructures incorporating inclined sidewalls is the vertical coupling of light into wave guide structures using a 45° prism [61]. Such optical devices must have a wall roughness of less than 50 nm, making LIGA a preferred technique for this application. The sharp decrease of the dose in the resist underneath the edge of the inclined absorber and the resulting sharp decrease of the dissolution of the resist as a function of the molecular weight in the developer result in little or no deviation of the inclination of the resist sidewall over the total height of the microstructure.

HANSER

Precision Injection Molding

Jehuda Greener, Reinhold Wimberger-Friedl

Process, Materials and Applications

ISBN 3-446-21670-7

Preface

Without a doubt, the unprecedented advances in consumer electronics and information technology over the last three decades were greatly facilitated by innovative plastics technologies that provided the low cost and performance needed to make the new products affordable and appealing to the average consumer. The watershed event that ushered the new era in the plastics industry was the introduction of the Compact Disc (CD) in 1982 following a joint development by Sony and Philips Corporations. This product revolutionized the music industry but in order for it to be successful in the marketplace, it had to be inexpensive and rugged. This need led to a complete overhaul and reinvention of the traditional injection molding process—the manufacturing technology of choice for this demanding new product. The injection molding of Compact Discs and many components of the CD system required new ways of looking at machine design, mold design, process control, material selection, product specification, and manufacturing technology. The conventional molding process, usually associated with "low-tech" applications, had to be adapted to the demanding tolerances and specifications of the microelectronics industry. Since then many consumer and commercial electronic devices and components (e.g., cell phones, digital cameras, mass storage devices, high precision biomedical components, microfluidic systems, and various optical components among others) have relied on high-precision molding operations for cost-effective manufacturing.

In this volume we bring together leading experts to address key technical issues that are directly associated with precision injection molding. The treatment covers many aspects of the technology, including materials, process, software, and hardware. It is not, however, meant to be comprehensive or exhaustive, but rather it is intended to present the status of current understanding for a broad range of issues, both fundamental and applied, that are important in the molding of high precision components. We also make the case that precision injection molding is a distinct subclass of the conventional and heavily studied injection molding process, with well-defined design, optimization and processability criteria.

We wish to thank our editor Christine Strohm, Shannon Kelly Proulx, and all the authors of this volume for their patience and understanding in allowing two very busy industrial scientists to oversee such a challenging project to its completion.

Jehuda Greener
Rochester, NY
USA

Reinhold Wimberger-Friedl
Eindhoven
The Netherlands

March 2006